JOURNAL OF VIROLOGY, Mar. 2005, p. 2754–2767 Vol. 79, No. 5
0022-538X/05/$08.00+0 doi:10.1128/JVI.79.5.2754–2767.2005

Human Cytomegalovirus Labeled with Green Fluorescent Protein for Live Analysis of Intracellular Particle Movements

Kerstin Laib Sampaio,[1] Yolaine Cavignac,[1] York-Dieter Stierhof,[2] and Christian Sinzger[1]*

Institute of Medical Virology[1] and Center for Plant Molecular Biology,[2] University of Tübingen, Tübingen, Germany

Received 23 January 2004/Accepted 12 October 2004

Human cytomegalovirus (HCMV) replicates in the nuclei of infected cells. Successful replication therefore depends on particle movements between the cell cortex and nucleus during entry and egress. To visualize HCMV particles in living cells, we have generated a recombinant HCMV expressing enhanced green fluorescent protein (EGFP) fused to the C terminus of the capsid-associated tegument protein pUL32 (pp150). The resulting UL32-EGFP-HCMV was analyzed by immunofluorescence, electron microscopy, immunoblotting, confocal microscopy, and time-lapse microscopy to evaluate the growth properties of this virus and the dynamics of particle movements. UL32-EGFP-HCMV replicated similarly to wild-type virus in fibroblast cultures. Green fluorescent virus particles were released from infected cells. The fluorescence stayed associated with particles during viral entry, and fluorescent progeny particles appeared in the nucleus at 44 h after infection. Surprisingly, strict colocalization of pUL32 and the major capsid protein pUL86 within nuclear inclusions indicated that incorporation of pUL32 into nascent HCMV particles occurred simultaneously with or immediately after assembly of the capsid. A slow transport of nuclear particles towards the nuclear margin was demonstrated. Within the cytoplasm, most particles performed irregular short-distance movements, while a smaller fraction of particles performed centripetal and centrifugal long-distance movements. Although numerous particles accumulated in the cytoplasm, release of particles from infected cells was a rare event, consistent with a release rate of about 1 infectious unit per h per cell in HCMV-infected fibroblasts as calculated from single-step growth curves. UL32-EGFP-HCMV will be useful for further investigations into the entry, maturation, and release of this virus.

Like all herpesviruses, human cytomegalovirus (HCMV) replicates in the nucleus of the infected cell (18). This aspect of the herpesviral replication strategy entails the requirement for various particle movements during the replicative cycle, in particular translocation of penetrated virus particles from the cell cortex towards the nucleus, egress of newly synthesized virus particles out of the nucleus, and translocation of tegumented and enveloped virus progeny towards the periphery of the cell in order to release infectious virus to surrounding cells (5, 14, 17, 19, 28). For HCMV, the importance of intracellular transport of virus particles was underscored by the finding that cell tropism variants of HCMV are discriminated by the strain-dependent efficiency of nuclear translocation (25). By nature, translocation is a dynamic process, which can be analyzed only insufficiently by biochemical analyses of lysates of infected cells or by immunodetection of particles in fixed-cell preparations. At least the dynamic aspects of interactions between virus particles and target cells are best studied in live-imaging approaches that have been enabled by the development of green fluorescent virus variants. Recombinant fluorescent viruses have been reported for herpes simplex virus and pseudorabies virus, the live imaging of which provided new insights into the nature of particle movements within relevant target cells (4, 6, 12, 21, 22, 27). Green fluorescent cytomegalovirus has also been reported (8, 10, 11, 16, 20, 23, 30); however, to date only nonstructural proteins have been tagged, and therefore these variants did not produce green fluorescent progeny virions. Live images of interactions between HCMV particles and their target cells are therefore not available to date. In order to obtain fluorescence tags that stay associated with HCMV particles during various intracellular translocation steps, the fluorescent protein has to be fused to viral capsid proteins or capsid-associated tegument proteins. One tegument protein known to be strongly associated with the capsid is the phosphoprotein pp150 (pUL32) (1, 2). Here we report the successful generation of a recombinant HCMV variant with enhanced green fluorescent protein (EGFP) fused to the C-terminal end of pUL32, resulting in green fluorescent virus particles. Possible applications of this green fluorescent HCMV variant include analyses of viral entry, nuclear translocation, nuclear egress after viral replication, dynamics of tegumentation, and viral egress. Examples of such applications are given in this study.

* Corresponding author. Mailing address: Institut für Medizinische Virologie, Universität Tübingen, Elfriede-Aulhorn-Strasse 6, D-72076 Tübingen, Germany. Phone: 7071 2987459. Fax: 7071 295790. E-mail: christian.sinzger@med.uni-tuebingen.de.

MATERIALS AND METHODS

Cells and viruses. All experiments were carried out with human foreskin fibroblasts (HFF) isolated from foreskins of infants by trypsin treatment and were used for experiments at passage 10 to 25. HFF were cultured in minimal essential medium (MEM) (Gibco, Karlsruhe, Germany) containing 5% fetal calf serum, 2.4 mmol of glutamine per liter, and 100 μg of gentamicin per ml (MEM5).

HCMV strain TB40 (26) was used for the generation of recombinant UL32-EGFP-HCMV. For the preparation of virus stocks, HFF were infected at a multiplicity of infection (MOI) (infectious units per cell) of 0.1. Supernatants of infected cultures were harvested at 6 days postinfection (p.i.) and stored at −80°C after removal of cell debris by centrifugation for 10 min at 2,800 × *g*. The infectious titer in HCMV preparations was determined by 50% tissue culture infective dose ($TCID_{50}$) assays (15) in HFF on 96-well plates. For supernatant-mediated infection of cell cultures, the medium was replaced by infectious

supernatant at the indicated MOI, incubated for 2 h at 37°C, and finally replaced with fresh medium (MEM5).

For single-step and multistep growth curves, HFF seeded in six-well plates (5×10^5 cells per well) were infected with cell-free HCMV preparations at a virus concentration of 2.5×10^5 $TCID_{50}$s/ml (MOI = 1) or 2×10^4 $TCID_{50}$s/ml (MOI = 0.08), respectively. After 2 h of incubation, the cultures were washed six times with medium to remove residual virus and were then cultured for 10 or 16 days, respectively. Starting at day 1 p.i., supernatant was removed daily from infected cultures and replaced by fresh medium; the supernatant samples were centrifuged at 2,800 × *g* for 10 min and stored at −80°C prior to determination of the infectious titer by $TCID_{50}$ assay.

For analysis of virus adsorption, cells were infected with virus preparations at 4°C for the indicated time intervals.

The EGFP-tagged recombinant HCMV described in this publication will be available at the American Type Culture Collection as ATCC VR1578.

Construction of the recombination plasmid. Genomic DNA was prepared from late-stage infected cells (4 days p.i.) by phenol-chloroform extraction. The complete HCMV-UL32 open reading frame, excluding the stop codon, was amplified by PCR with the oligonucleotides 5′-C**GGATCC**TCCGTGTTCTTAA TCTTCTCGA and 3′-AA**GCTAGC**ATGAGTTTGCAGTTTATCGGTC, which were partial mismatch primers changing the last amino acid of pUL32 from Glu (E) to Asp (D) and introducing one BamHI site and one NheI site at the ends of the amplification product. The amplification product was cloned into the PCR cloning vector pDrive (Qiagen, Hilden, Germany). The BamHI/NheI fragment containing the UL32 open reading frame was excised by using the restriction sites integrated into the primers (indicated by boldface) and was then cloned into the BamHI/NheI site of the EGFP-N1 vector (BD Clontech, Heidelberg, Germany). The resulting UL32-EGFP open reading frame contains five additional codons between the last UL32 codon and the first EGFP codon. To obtain a recombination plasmid, a 1.6-kbp fragment containing part of the UL31 open reading frame was amplified by PCR with the oligonucleotides 5′-AA**CTTAAG**GAGG GGAGACGAGGACGACAGG and 3′-GG**TCTAGA**AACACACACGCAGAC GTACTTT, which were partial mismatch primers introducing one AflII site and one XbaI site at the ends of the amplification product. The PCR products were cloned into the PCR cloning vector pDrive (Qiagen). AflII/XbaI fragments containing part of the UL31 sequence were excised by using the restriction sites integrated into the primers (indicated by boldface), and the UL31 fragment was cloned into the AflII/XbaI site of the UL32-EGFP construct. This resulted in a recombination plasmid that was suitable for introduction of a pUL32-EGFP fusion gene at the orthotopic site of the HCMV genome by homologous recombination. This recombination plasmid was designated UL32-EGFP/UL31.

Generation and plaque purification of recombinant HCMV. The UL32-EGFP recombination plasmid UL32-EGFP/UL31 was cleaved with NheI and AflII, ethanol precipitated, and dissolved in H_2O. The cleaved construct was microinjected into the nuclei of HCMV-TB40-infected HFF at 2 days p.i. by using a micromanipulation system (InjectMan and Femtojet; Eppendorf, Hamburg, Germany). At 4 days p.i. cells were cocultured with noninfected HFF at a ratio of 1/2,000 in 96-well plates and screened subsequently for EGFP-expressing foci of infected cells. Virus supernatant from wells containing green fluorescent foci was plaque purified three times by limiting-dilution infections in 96-well plates with centrifugal enhancement. To enrich for recombinant virus, wells that displayed single standing green fluorescent foci were preferred for the subsequent step of purification. A virus preparation was considered pure when all foci resulting from limiting-dilution infections with this preparation displayed EGFP expression, indicating that no wild-type virus remained in the preparation. In brief, this was tested by acetone fixation of the respective 96-well plate followed by double immunofluorescence against pUL32 and EGFP. The viral tegument protein pUL32 was detected by using monoclonal antibody (MAb) XP1 (Dade Behring, Schwalbach, Germany) and Cy3-labeled goat anti-mouse immunoglobulin (Ig) antibodies (Jackson ImmunoResearch, West Grove, Pa.), resulting in red fluorescence. The EGFP fusion part of the pUL32-EGFP protein was detected by using polyclonal antibody (PAb) ab290 (rabbit; Abcam, Cambridge, United Kingdom) and Alexa Fluor488-labeled goat anti-rabbit Ig antibodies (Molecular Probes, Eugene, Oreg.), resulting in green fluorescence. While staining of pUL32 detected all HCMV-infected foci, staining of EGFP documented that the focus contained recombinant virus.

Gradient purification of HCMV virions. For gradient purification of HCMV virions, infectious supernatants from infected HFF cultures with ≈100% late-stage cytopathic effects were made cell free by centrifugation for 10 min at 2,800 × *g*. Supernatants were then ultracentrifuged for 70 min at 80,000 × *g*. Pellets containing virions and other particles were resuspended in 1 ml of phosphate-buffered saline (PBS) and transferred onto a preformed linear glycerol-tartrate gradient (15 to 35% Na-tartrate and 30 to 0% glycerol in 0.04% Na-phosphate), which was then ultracentrifuged for 45 min at 80,000 × *g*. The virion-containing band was harvested with a syringe, and the virions were washed and pelleted by an additional ultracentrifugation for 70 min at 80,000 × *g*. The pellet was resuspended in MEM5 and stored at −80°C until used for infection experiments.

Immunoblotting. Virus particles were prepared from cell-free supernatants of infected HFF cultures with ≈100% late-stage cytopathic effects by ultracentrifugation at 80,000 × *g* for 70 min. Pellets were lysed in sample buffer containing 2% sodium dodecyl sulfate and 5% β-mercaptoethanol, and proteins were denatured at 95°C for 10 min, separated by sodium dodecyl sulfate-12% polyacrylamide gel electrophoresis, and blotted onto nitrocellulose. Detection was done with anti-pUL32 MAb (XP1; Dade Behring), followed by incubation with peroxidase-conjugated polyclonal rabbit anti-mouse Ig sera (Dako, Hamburg, Germany). Proteins were visualized with the Super Signal West Pico chemiluminescence substrate (Pierce, Rockford, Ill.), using a Fluor-S MAX Multiimager (Bio-Rad, Munich, Germany).

Immunofluorescence. To analyze the kinetics of viral gene expression, MAbs against viral proteins from different phases of the replicative cycle of HCMV were used. In detail, MAbs were directed against the immediate-early (IE) proteins IE72 and IE86 (pUL122/123, MAb E13; Biosoft, Paris, France), the early protein p52 (pUL44, MAb BS510; Biotest, Dreieich, Germany), and the late major capsid protein (pUL86, MAb 28–4; kindly provided by W. Britt, Birmingham, Ala.). For colocalization studies, primary antibodies against the late tegument protein pp150 (pUL32, MAb XP1; Dade Behring) and the EGFP protein (PAb ab290 [Abcam] and PAb TP401 [Torrey Pines Biolabs, Houston, Tex.]) were used.

For in situ detection of antigens in infected cells, indirect immunofluorescence was done as follows. At various time points after infection, infected cells grown on 96-well plates (μclear; Greiner, Frickenhausen, Germany) were fixed with 80% acetone for 5 min at room temperature. The fixed cells were reacted with primary antibodies for 60 min at 37°C, followed by incubation with fluorescent secondary antibodies for 60 min at 37°C. To obtain red fluorescent signals, Cy3-conjugated goat anti-mouse IgG $F(ab')_2$ or Cy3-conjugated goat anti-rabbit IgG $F(ab')_2$ fragments (Jackson ImmunoResearch) were used as secondary antibodies. To obtain green fluorescent signals, Alexa Fluor488-conjugated goat anti-mouse IgG $F(ab')_2$ or Alexa Fluor488-conjugated goat anti-rabbit IgG $F(ab')_2$ fragments (Molecular Probes) were used as a secondary antibodies.

For simultaneous detection of pUL32-EGFP and the nuclear membranes of infected cells, indirect-immunofluorescence stainings were analyzed in a confocal laser scanning microscope (TCS SP2; Leica Mikrosysteme, Bensheim, Germany). A cell suspension containing infected fibroblasts at 3 days p.i. in MEM5 was dropped on coverslips and allowed to adhere for 1 h at 37°C. The adherent cells were fixed with 100% acetone for 5 min at room temperature. The fixed cells were reacted with a mixture of MAb AB-1 against lamin B (Calbiochem, Cambridge, Mass.) and PAb ab290 against EGFP (Abcam) for 60 min at 37°C, followed by incubation for 60 min at 37°C with a mixture of Cy3-conjugated goat anti-mouse IgG $F(ab')_2$ fragments (Jackson ImmunoResearch) and Alexa Fluor488-conjugated goat anti-rabbit IgG $F(ab')_2$ fragments (Molecular Probes).

For simultaneous detection of pUL32-EGFP and the HCMV major capsid protein pUL86, confocal laser scanning microscopy was performed as follows. A cell suspension containing infected fibroblasts at 4 days p.i. in MEM5 was dropped on coverslips and allowed to adhere for 1 h at 37°C. The adherent cells were fixed with 1% paraformaldehyde for 10 min at room temperature and permeabilized with 0.5% Igepal, 10% sucrose, and 1% fetal calf serum for 5 min at room temperature. The fixed cells were reacted with MAb 28–4 against HCMV pUL86 (kindly provided by W. Britt) for 60 min at 37°C, followed by incubation for 60 min at 37°C with Cy3-conjugated goat anti-mouse IgG $F(ab')_2$ fragments (Jackson ImmunoResearch). Finally, cell nuclei were stained with DAPI (4′,6′-diamidino-2-phenylindole). The red fluorescence signal of the capsid protein pUL86, the native green fluorescence of pUL32-EGFP, and the blue fluorescence of DAPI were then detected separately and merged by using Leica confocal software.

Transmission electron microscopy. Fibroblast monolayer cells were fixed with 4% formaldehyde in PBS (pH 7.2) for 30 min on ice, followed by treatment with 8% formaldehyde in PBS for another 120 min on ice. Fixed cells in the culture flask were scraped off, infiltrated with 2.1 M sucrose in PBS, and frozen in liquid nitrogen, and then 100-nm-diameter cryosections were obtained with a Leica Ultracut UCT/EM FCS cryo-ultramicrotome at −100°C. Thawed cryosections were blocked with 1% milk powder–0.5% bovine serum albumin in PBS and incubated with rabbit anti-GFP (1:200; Torrey Pines Biolabs) or mouse monoclonal anti-HCMV pUL32 antibodies (1:5; Dade Behring) in blocking buffer for 60 min. After washing with blocking buffer, bound antibodies were detected with goat anti-rabbit or goat anti-mouse IgG coupled to Nanogold (Nanoprobes) or ultrasmall gold (Aurion). Silver enhancement was performed as described by

Danscher (3) and by Stierhof et al. (29). Final embedding was done in 2% methyl cellulose containing 0.3% uranyl acetate. Ultrathin sections were viewed in a LEO 906 transmission electron microscope.

PCR assay. DNA was prepared by phenol-chloroform extraction from HCMV-infected HFF with ≈100% cytopathic effect. The probe was diluted to a total DNA concentration of 0.6 μg/ml. Viral nucleic acids within these probes were amplified by PCR with primers P1, located within UL32 (5′-TGT GGC CTC CCC CTC CAT CCT GAA A-3′), and P2, located within UL31 (5′-ACC GGT GTT TCT TGG TGG CCA ACT T-3′). Primers were designed to amplify a 634-bp fragment within the wild-type HCMV genome and a 1,378-bp fragment within the genome of the recombinant HCMV strain UL32-EGFP-HCMV-TB40 due to the insertion of the EGFP open reading frame. The reactions were done in a total volume of 50 μl consisting of 1.5 mmol of $MgCl_2$, 0.25 mmol of each deoxynucleoside triphosphate, 10 pmol of each primer, 1× PCR buffer, and 1 U of *Taq* polymerase (Roche Diagnostics GmbH, Mannheim, Germany). Thermal cycling was performed as follows with 35 cycles of 94°C for 1 min, 57°C for 1 min, and 72°C for 1 min. Amplification products were visualized by electrophoresis in agarose gels, ethidium bromide staining, and UV light exposure.

Live imaging. Cells for live analysis were cultured on 35-mm-diameter glass-bottom dishes (MatTek, Ashland, Mass.) or on 96-well plates (μclear; Greiner). For analysis of virus entry, infectious supernatant containing green fluorescent virus was prepared freshly from late-stage infected cells at 5 days p.i. Alternatively, gradient-purified virion particles were used for infections. In order to reduce the fluorescence background, medium without phenol red was used. In order to minimize the presence of biologically inactive virions, the medium was refreshed 24 h prior to harvest of supernatant. Cells were incubated with undiluted supernatant for 1 h at 37°C and subsequently washed six times to remove nonadherent virus particles. In these experiments, the cell culture medium was supplemented with 1 mmol of ascorbic acid per liter, 40 U of glucose oxidase per ml, and 800 U of catalase per ml to reduce the cytotoxic effects of free radicals in solution during imaging. When desired, nuclei of living cells were stained by addition of DAPI to the culture medium. To study the kinetics of the appearance of UL32-EGFP-HCMV particles, cells were infected with fresh virus supernatant at a low dose (MOI = 0.05), resulting in ≤3 input virus particles/cell. Infected cultures were subsequently monitored for the appearance of green fluorescent cells. When punctate fluorescence signals started to increase, individual cells were chosen for serial photodocumentation over a period of several hours. To study particle movements during the productive phase of viral replication, cells were infected at an infection efficiency of 10% and analyzed at 4 days p.i. over time periods of 300 s. For a descriptive statistical analysis of particle movements, each 50 events of centripetal and centrifugal movements were evaluated in regard to the velocity and distance of the movement. A movement event was defined as an uninterrupted translocation of >2 μm in length.

Prior to analysis, dishes were placed in a humidified chamber supplied with 5% CO_2 (M200 incubator controlled by a CTI-Controller 3700 and a Tempcontrol 37–2; Carl Zeiss, Göttingen, Germany) that was mounted on an Axiovert 200 inverted fluorescence microscope (Carl Zeiss) and was heated to 37°C. Images at individual time points were taken at an excitation wavelength of 450 to 490 nm with an Axiocam MRm digital camera (Carl Zeiss) controlled by Axiovision 3.1 software. Punctate signals of higher fluorescence intensity on the background of a homogeneous moderate fluorescence pattern represented viral particles.

RESULTS

Growth of recombinant UL32-EGFP-HCMV in human foreskin fibroblasts. Generation of EGFP-labeled HCMV was done by homologous recombination in order to cause minimal alteration of the genomic content at the recombination site (Fig. 1A), thus avoiding impairment of viral growth by effects other than the EGFP labeling of pUL32 itself. For homologous recombination, a plasmid was constructed that fused the complete EGFP open reading frame to the C terminus of the UL32 open reading frame of HCMV strain TB40, from which only the last codon was removed. Due to the cloning strategy, one amino acid exchange (K1054H) appeared at the C terminus of the UL32 open reading frame, and six amino acids, encoded by the multiple cloning site of the EGFP cloning vector, were inserted between the C terminus of UL32 and the N terminus of EGFP. The C terminus of the EGFP open reading frame was then flanked by 1,622 nucleotides of the adjacent UL31 open reading frame in order to allow for homologous recombination at the orthotopic site of the HCMV genome. Microinjection of the recombination plasmid UL32-EGFP/UL31 into HCMV-TB40-infected fibroblasts 2 days after infection resulted in growth of recombinant UL32-EGFP-HCMV-TB40, which was enriched by three subsequent plaque purifications. The purity of the resulting virus preparation was confirmed by limiting-dilution infections of fibroblast cultures and subsequent simultaneous immunofluorescence staining for HCMV-pUL32 and EGFP. All infected cells expressed pUL32 and EGFP in perfect colocalization (Fig. 1B). No cell that expressed pUL32 without expressing EGFP was detected, thus indicating that plaque-purified preparations of UL32-EGFP-HCMV-TB40 were free of any contaminating wild-type virus. The sequence of the EGFP-flanking regions in the purified recombinant virus strain UL32-EGFP-HCMV-TB40 was determined (Fig. 1A), and this proved that the recombination had occurred at the correct site.

The growth properties of UL32-EGFP-HCMV-TB40 were tested by immunofluorescence analyses of viral antigen expression and by quantitative detection of virus progeny released from infected fibroblast cultures. Viral IE, early, and late antigens became detectable at 2, 24, and 48 h p.i., respectively (Fig. 2A), thus closely resembling the antigen expression kinetics of wild-type HCMV. In single-step and multistep growth curves, UL32-EGFP-HCMV-TB40 behaved identically to wild-type HCMV with regard to the kinetics and maximum titers of progeny virus (Fig. 2B and C). Furthermore, the localization of pUL32-EGFP in cells infected by UL32-EGFP-HCMV-TB40 was identical to the localization of pUL32 in cells infected by wild-type HCMV-TB40, thus ruling out the possibility that green fluorescent signals observed during live analyses could originate from EGFP polypeptides that might have been cleaved from the pUL32-EGFP protein (Fig. 2D).

Although we cannot exclude slight differences in the level of UL32 expression between wild-type virus and the recombinant virus, there were at least no obvious differences in the pUL32 immunofluorescence patterns with regard to localization and signal strength.

In conclusion, a recombinant UL32-EGFP-HCMV-TB40 was generated, which expressed green fluorescent pp150 from the UL32 gene located in the orthotopic position. This recombinant virus did not differ from wild-type HCMV-TB40 with regard to protein expression and viral growth.

Release of green fluorescent virus particles by UL32-EGFP-HCMV-infected cells. In order to test whether the green fluorescent pUL32 was actually incorporated in progeny virus particles of UL32-EGFP-HCMV-TB40, we further analyzed the supernatants of infected-cell cultures. Cell-free preparations harvested from infected fibroblasts at 7 days p.i. were incubated with freshly seeded fibroblasts for 2 h at 4°C, a condition that is known to allow for virus adsorption only. A concentration-dependent punctate cell surface pattern of green fluorescence was detected, resembling the pattern described previously after pUL32 immunostaining of fixed cells infected under the same conditions (Fig. 3A) (25). Identical patterns of green punctate fluorescence were obtained when adsorption experiments were repeated with highly concentrated purified UL32-EGFP-HCMV-TB40 virion particles harvested from glycerol-

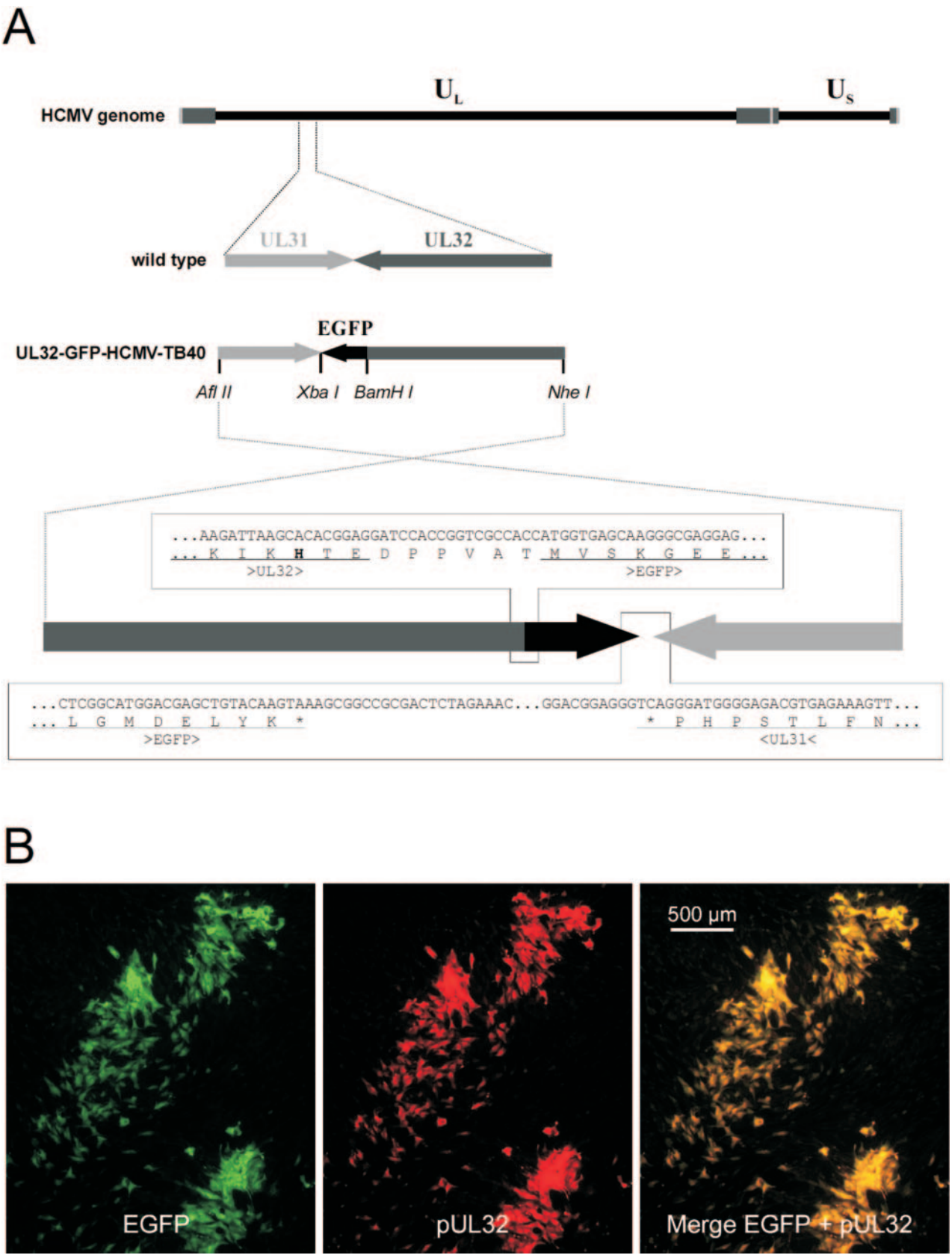

FIG. 1. (A) Flow chart of the generation of recombinant UL32-EGFP-HCMV-TB40. The boldface letter in the sequence indicates the amino acid exchange (K1054H) at the C terminus of the UL32 open reading frame. (B) Colocalization of pUL32 (red) and EGFP (green) detected by indirect-immunofluorescence assays in viral plaques after infection of fibroblasts with plaque-purified UL32-EGFP-HCMV-TB40.

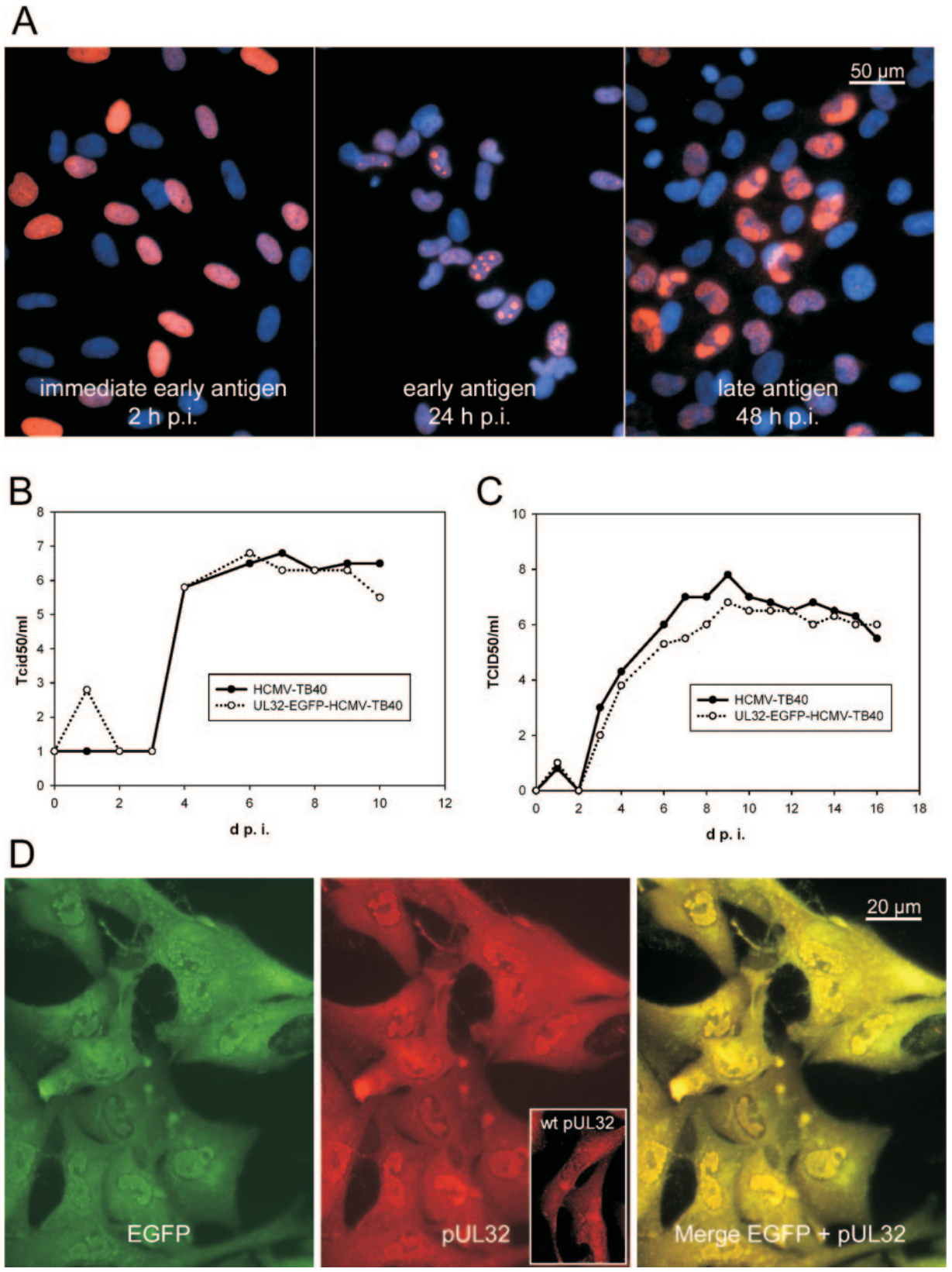

FIG. 2. Growth of recombinant UL32-EGFP-HCMV-TB40 in human foreskin fibroblasts. (A) Kinetics of viral antigen expression. Viral immediate-early antigen (pUL122/123), early antigen (pUL44), and late antigen (pUL86) were detected in infected fibroblasts by indirect immunofluorescence. The first time point of appearance is indicated. (B) Single-step growth curves of wild-type HCMV strain TB40 and the recombinant HCMV strain UL32-EGFP-HCMV-TB40. Fibroblast cultures were infected at an MOI of 1, and infectious virus progeny in the

tartrate gradients (MOI = 500), thus indicating that green fluorescent pUL32 is incorporated in infectious virions (Fig. 3B). After infection with green fluorescent UL32-EGFP-HCMV-TB40 particles, viral IE antigens were expressed as indicated by indirect immunofluorescence of fixed cells (results were identical to those in Fig. 2A), thus proving the infectivities of the respective virion preparations. On a single-particle level, pUL32 signals and GFP signals were almost perfectly colocalized in cells infected by UL32-EGFP-HCMV-TB40, whereas cells infected by wild-type HCMV-TB40 showed only pUL32 signals (Fig. 3C). In coinfection experiments, the two strains could thus be discriminated (Fig. 3C).

The question of whether EGFP signals actually represent virion particles was addressed by immunogold labeling of EGFP and subsequent electron microscopy. Fibroblasts were infected with highly concentrated gradient-purified UL32-EGFP-HCMV-TB40 virion particles for 30 min. Ultrathin cryosections were labeled with anti-GFP antibodies and silver-enhanced ultrasmall gold and were analyzed by electron microscopy. This ultrastructural analysis demonstrated that pUL32-EGFP is a component of virions and that single virion particles but not aggregates of virions were attached to cells (Fig. 3D). Additional proof of incorporation of pUL32-EGFP into virus particles was obtained by comparative Western blot analyses of cell-free virus particles from UL32-EGFP-HCMV-TB40 and wild-type HCMV-TB40. When immunoblotting was performed with monoclonal antibodies directed against pUL32, a single band was detected with both virus preparations (Fig. 3E). Compared to wild-type virus, the pUL32 signal of UL32-EGFP-HCMV-TB40 was shifted to a higher apparent molecular weight, concordant with the assumption of fusion of EGFP to pUL32. No wild-type pUL32 signal was detected in UL32-EGFP-HCMV-TB40 preparations, further emphasizing the purity of the recombinant virus. The final proof of the purity of plaque-purified UL32-GFP-HCMV-TB40 was given by PCR assays with a primer set that allowed for amplification of a fragment reaching from the C terminus of UL32 to the C terminus of UL31. In wild-type virus the length of the resulting amplification product is 634 bp, whereas in the recombinant virus the amplification product was calculated to be 1,378 bp in length due to insertion of the complete EGFP open reading frame. PCR assays of DNA preparations from wild-type virus and recombinant virus displayed the expected shift in the fragment length and demonstrated that no wild-type amplification products could be generated from DNA preparations of plaque-purified UL32-EGFP-HCMV-TB40 (Fig. 3F).

Kinetics of appearance and intracellular localization of UL32-EGFP-HCMV particles during the replication cycle. When UL32-EGFP-HCMV-TB40 was found to produce infectious green fluorescent virions with growth properties identical to those of wild-type virus, the next step was to analyze at what time and at what localization green fluorescent HCMV particles can be detected during the replicative cycle. Live-imaging analyses were done by sequential photography of infected fibroblast cultures in a fluorescence microscope. Cells were infected at an MOI of 0.05 to ensure that they were infected by a low number of input virus particles. As expected, after adsorption and penetration, one to three virus particles were detected per cell. At 40 h after infection, infected cells displayed a homogenous cytoplasmic green fluorescence signal and a somewhat less intense nuclear green fluorescence signal. On the background of these diffuse cytoplasmic and nuclear fluorescence patterns, the more intense punctate signals of virus particles could be discriminated, but these cells still did not contain more than three punctate fluorescence signals, which might have originated from input virus. At 44 h p.i. the number of punctate signals per cell began to increase, indicating de novo generation of green fluorescent virus progeny. At that time point the punctate signals were located predominantly at the nucleus (Fig. 4A). Subsequently, the numbers of green fluorescent particles within the nucleus and cytoplasm continuously increased, and the pattern changed to a predominance of cytoplasmic accumulation of particles within several hours (Fig. 4B to D).

Although it could not be determined from fluorescence images whether "nuclear" particles were located inside the nucleus or at the nuclear membrane, the association of "nuclear" particles with nuclear inclusions at later time points suggested that at least part of these particles were located inside the nucleus. Not only were punctate fluorescence signals colocalized with nuclear inclusions as detected by phase-contrast microscopy, but nuclear inclusions also were always highlighted by a homogeneous fluorescence signal. A homogeneous distribution of the pUL32-EGFP protein in viral replication compartments combined with the appearance of green fluorescent particles at these sites suggested that nascent viral particles acquired the tegument protein pUL32 already in the nucleus (Fig. 4E). This was an unexpected finding, and therefore this aspect was further analyzed. For a more precise determination of the localization of particles, confocal laser scanning microscopy of pUL32-EGFP immunofluorescence signals versus lamin B immunofluorescence signals was performed. Numerous punctate pUL32 immunofluorescence signals were found within the nucleus (Fig. 4F), thus confirming the intranuclear localization of particles as already suggested by live analyses of green fluorescent particles. Intranuclear fluorescence signals of pUL32-EGFP were almost perfectly colocalized with immunofluorescence signals of the major capsid protein pUL86 (Fig. 4G), supporting the assumption that punctate fluorescence patterns did not reflect accumulations of the isolated pUL32-EGFP protein but actually represented tegumented virus particles. The ultrastructural localization of immunogold-labeled pUL32-EGFP in nuclear replication compartments (Fig. 4H) confirmed the immunofluorescence data by proving the association of pUL32-EGFP with nascent progeny virus capsids in the nucleus. When immunogold analyses were done with an-

supernatants of infected cultures was determined daily by limiting-dilution analyses. (C) Multistep growth curves of wild-type HCMV strain TB40 and the recombinant HCMV strain UL32-EGFP-HCMV-TB40. Fibroblast cultures were infected at an MOI of 0.08, and infectious virus progeny in the supernatants of infected cultures was determined daily by limiting-dilution analyses. (D) Subcellular colocalization of pUL32 (red) and EGFP (green) detected by indirect-immunofluorescence assays in infected fibroblasts 4 days after infection with UL32-EGFP-HCMV-TB40. For comparison, the inset displays subcellular localization of pUL32 (red) in infected fibroblasts 4 days after infection with wild-type (wt) HCMV-TB40.

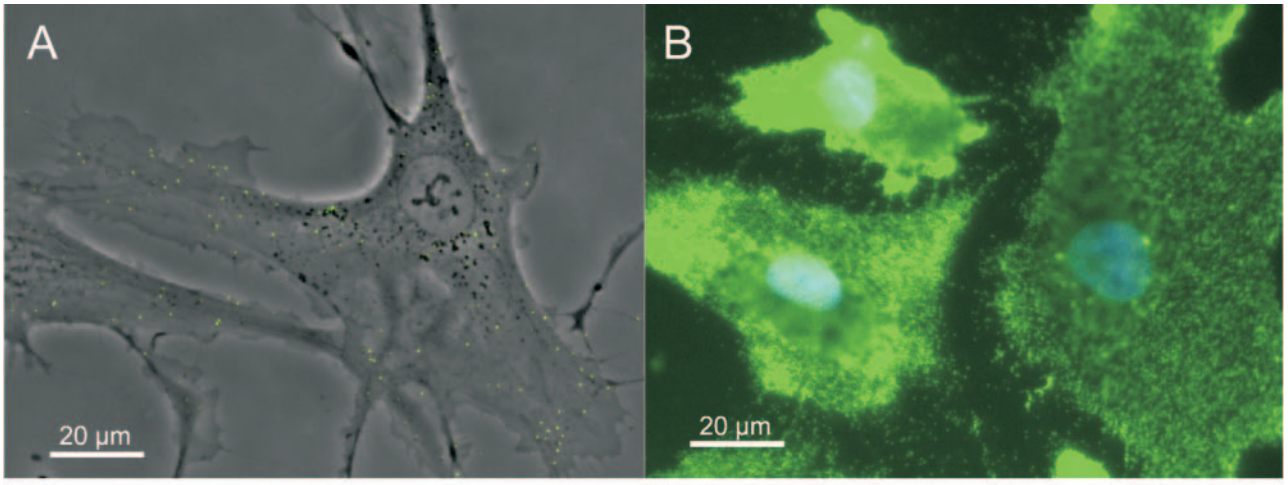
A
20 μm
B
20 μm

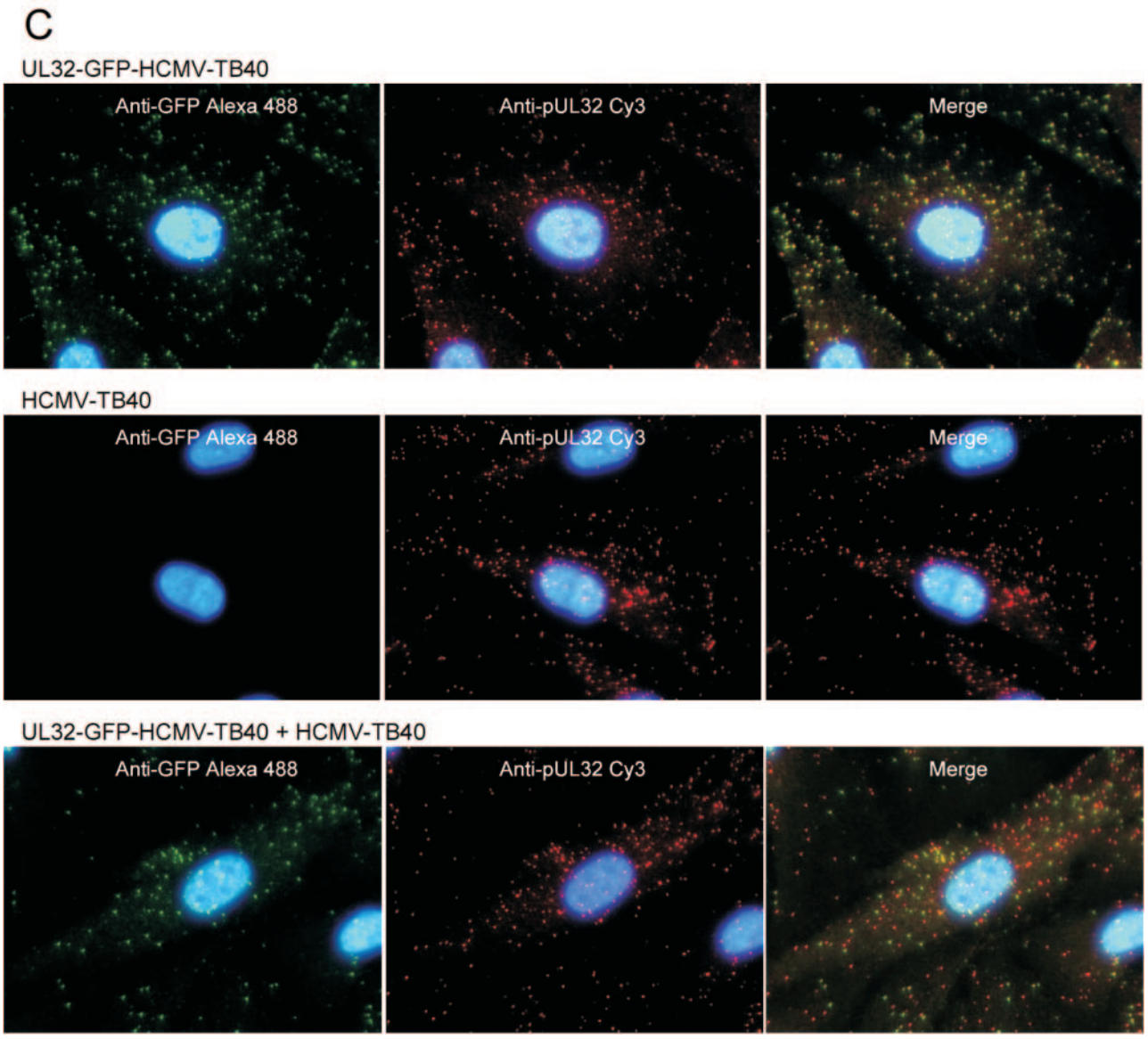
C
UL32-GFP-HCMV-TB40
Anti-GFP Alexa 488
Anti-pUL32 Cy3
Merge
HCMV-TB40
Anti-GFP Alexa 488
Anti-pUL32 Cy3
Merge
UL32-GFP-HCMV-TB40 + HCMV-TB40
Anti-GFP Alexa 488
Anti-pUL32 Cy3
Merge

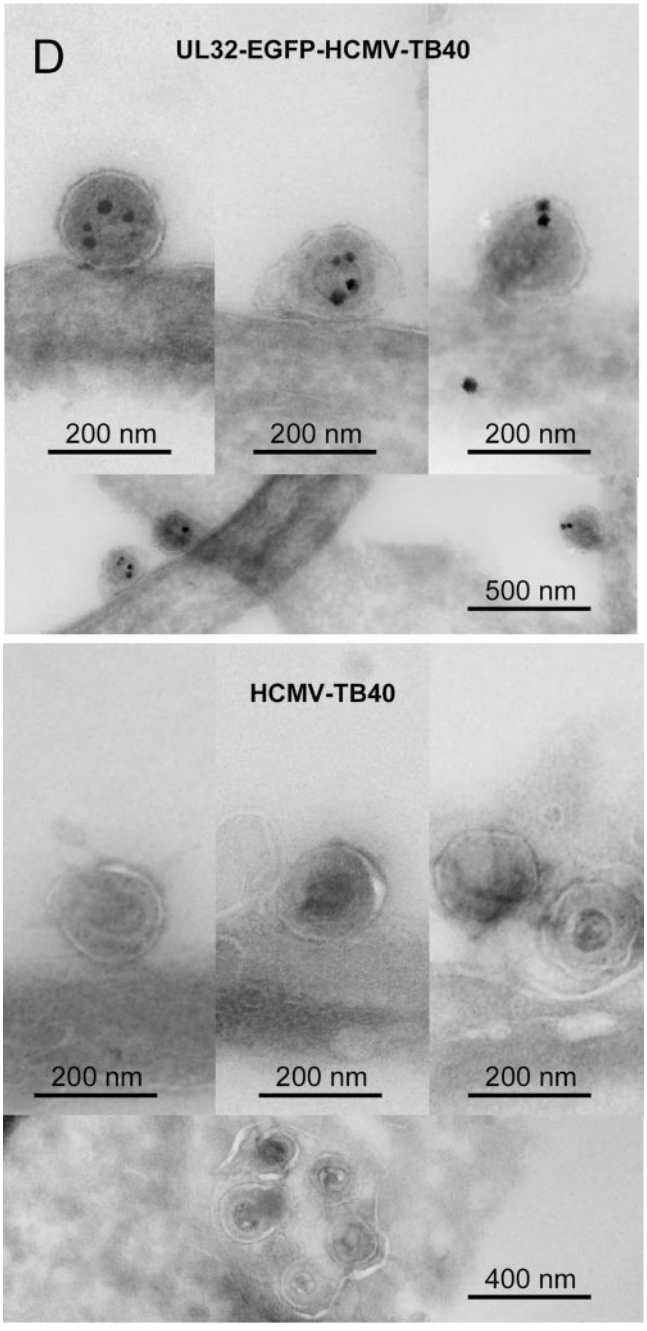

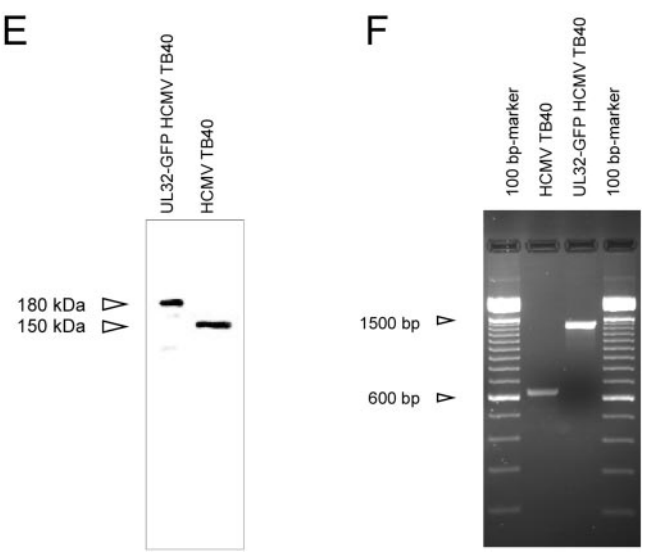

FIG. 3. Microscopic and biochemical analysis of green fluorescent virus UL32-EGFP-HCMV particles. (A) Detection of green fluorescent UL32-EGFP-HCMV-TB40 particles in cultured fibroblasts by merge of fluorescence and phase-contrast micrographs under conditions of viral adsorption. (B) Detection of gradient-purified UL32-EGFP-HCMV-TB40 virions in cultured fibroblasts by merge of fluorescence micrograph and DAPI stain under conditions of viral adsorption. (C) Detection of GFP and pUL32 in infected fibroblasts at 1 h after infection with UL32-GFP-HCMV-TB40 or HCMV-TB40 or a mixture of both virus strains. Almost all UL32-GFP-HCMV-TB40 particles are detected by the GFP antibody. In contrast, no wild-type particles are detected by the GFP antibody, proving the specificity of the staining. In coinfections, the different strains can by discriminated. (D) Ultrastructural localization of the pUL32-EGFP fusion protein after adsorption of gradient-purified UL32-EGFP-HCMV-TB40 virions or wild-type virions to cultured fibroblasts. EGFP was detected by immunogold labeling on ultrathin cryosections. (E) Immunoblotting of protein lysates of UL32-EGFP-HCMV-TB40-particles versus wild-type HCMV-TB40 particles, using a primary antibody against pUL32. (F) Detection of PCR amplification products specific for wild-type virus (634 bp) and recombinant virus (1,378 bp) in DNA preparations from wild-type HCMV-TB40 and recombinant UL32-EGFP-HCMV, using a primer pair spanning the UL31-UL32 transition region.

tibodies against pUL32 instead of anti-GFP antibodies, the results were identical (data not shown). The colocalization of pUL32-EGFP with capsids in nuclear replication compartments further indicated that incorporation of pUL32 into nascent HCMV particles occurred simultaneously with or immediately after assembly of the capsid.

Live imaging of particle movements in infected fibroblasts during the viral replication cycle. The dynamics of HCMV particle movements in infected HFF were then analyzed by sequential fluorescence microscopic photography. To document the movements of single particles, time frames of 1, 2, or 4 s were chosen.

In general, almost all intracellular virus particles were in motion, irrespective of whether penetrated input virus or newly synthesized progeny virus was analyzed. The majority of moving particles performed small irregular movements in place, whereas only a small fraction performed saltatory movements of about 2 to 16 μm in length. Saltatory movements occurred in both centripetal and centrifugal directions at speeds of 0.79 (range, 0.24 to 1.82) and 0.76 (0.27 to 1.98) μm/s, respectively. The distance of single movement events was 6.96 (2.14 to 15.40) and 6.13 (2.75 to 16.30) μm, respectively (Fig. 5C). If particles performed multiple saltations in the same direction, long-distance translocations could result. If a certain particle performed saltations of alternating direction, this resulted in back-and-forth movements. As an exception, certain sites within the nuclear inclusion seemed to contain accumulations of stationary particles. The movement pattern within an infected cell seemed to be rather chaotic, and a predominating process could not be identified during any phase of viral replication.

In particular, we have investigated cells at 1 h p.i., at a stage

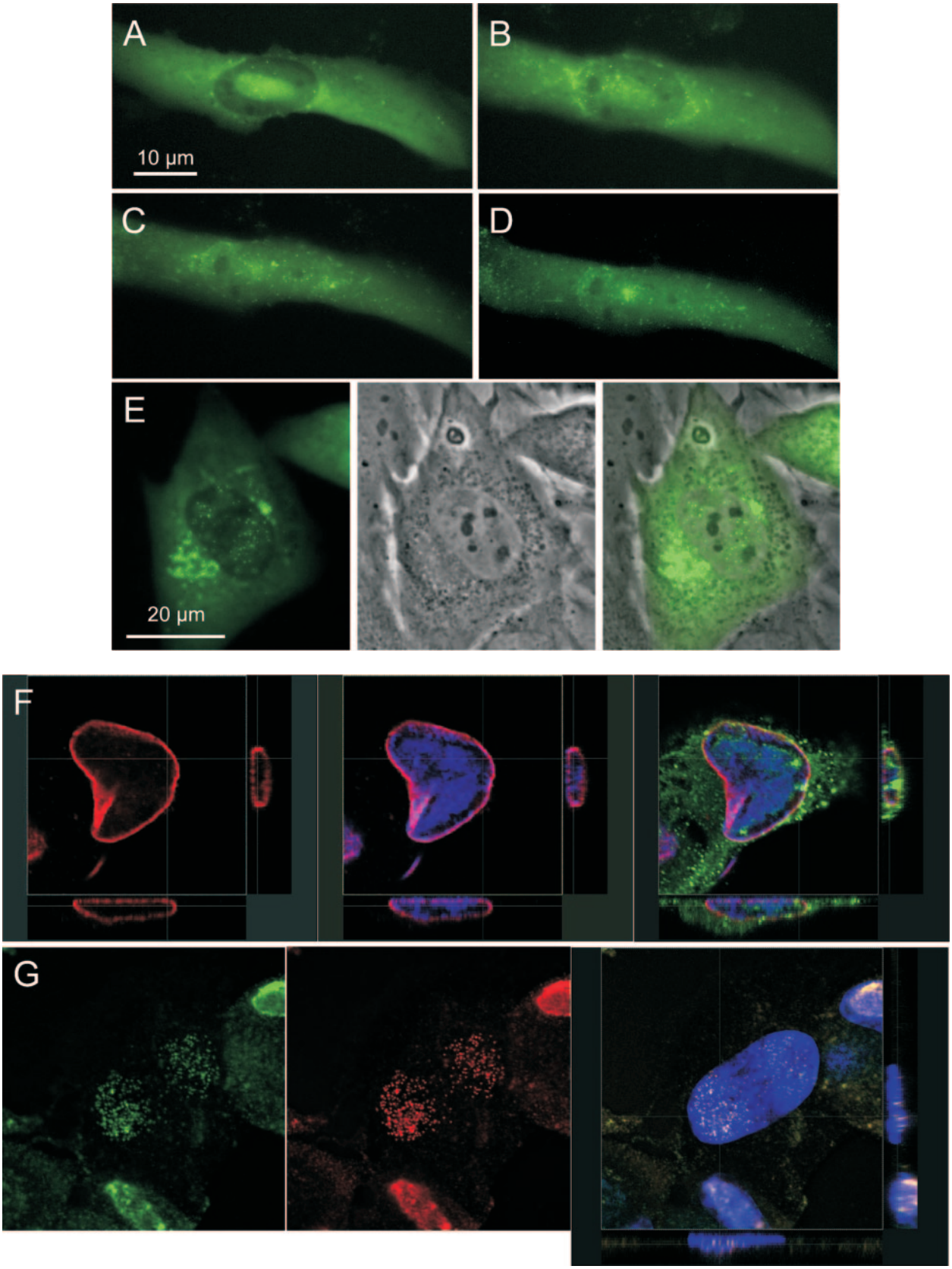

FIG. 4. Kinetics of appearance and intracellular localization of UL32-EGFP-HCMV-TB40 particles during the replication cycle. (A to D) Appearance of green fluorescent particles in a living infected fibroblast at 44 h (A), 48 h (B), 50 h (C), and 51 h (D) after infection at an MOI of 0.05. (E) Subcellular localization of green fluorescent particles displayed by an overlay of fluorescence microscopy and phase-contrast

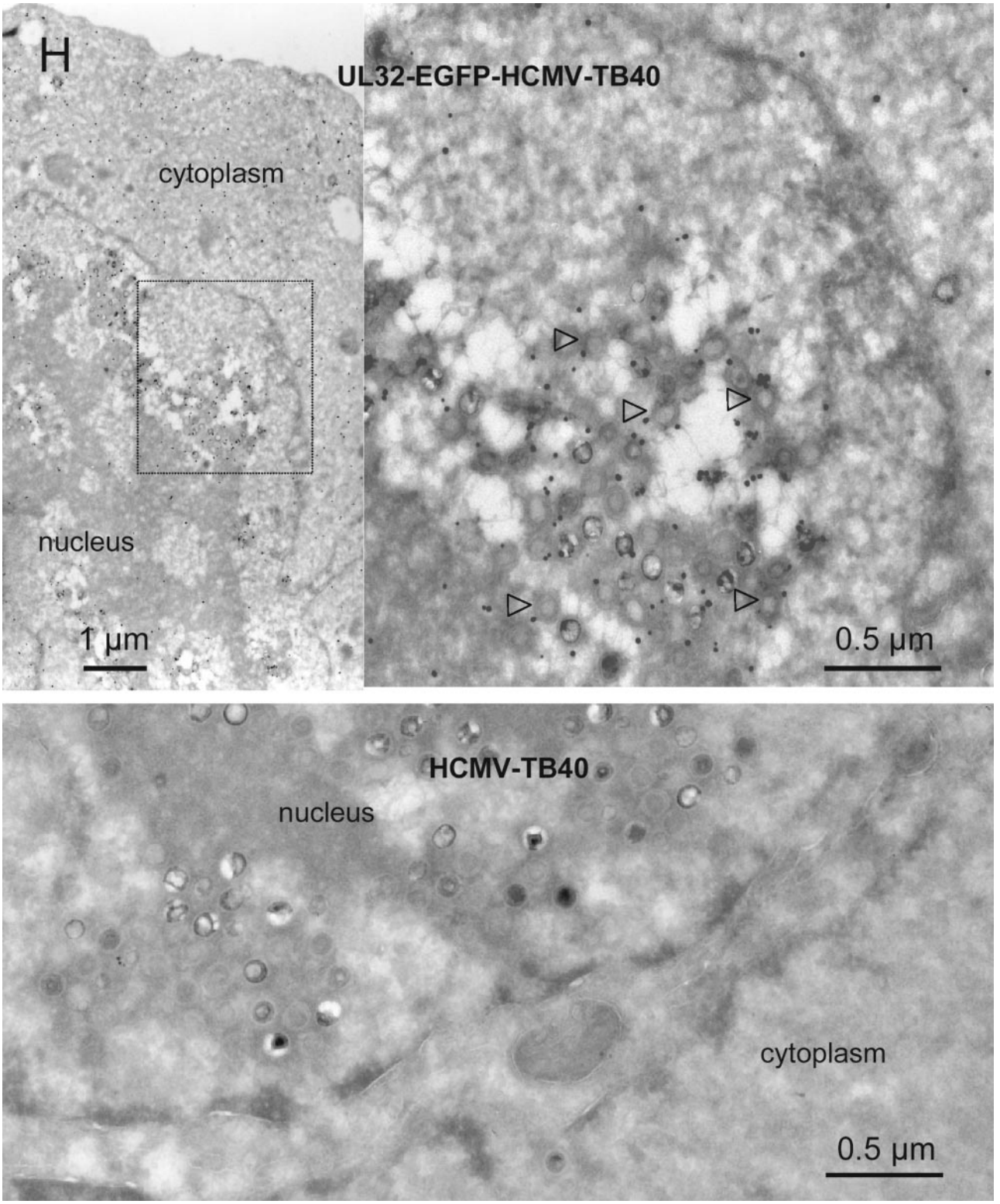

microscopy of a living infected cell at 65 h p.i. (F) Subcellular localization of green fluorescent particles as detected by confocal laser scanning microscopy of an acetone-fixed infected cell at 72 h p.i. Indirect immunofluorescence of lamin B (Cy3, red) and EGFP (Alexa 488, green) versus DNA staining (DAPI, blue) is shown. (G) Intranuclear colocalization of the tegument protein pUL32 and the major capsid protein pUL86 by confocal laser scanning microscopy of a paraformaldehyde-fixed infected cell at 72 h p.i. The native fluorescence of pUL32-EGFP is displayed versus indirect immunofluorescence of pUL86 (Cy3, red) and DNA staining (DAPI, blue). (H) Ultrastructural localization of the pUL32-EGFP fusion protein. Fibroblast cultures at 4 days after infection with UL32-EGFP-HCMV-TB40 or with wild-type virus were fixed and cryosectioned. EGFP was detected by immunogold labeling on ultrathin cryosections. Examples of viral capsids with associated pUL32-EGFP are indicated by arrowheads.

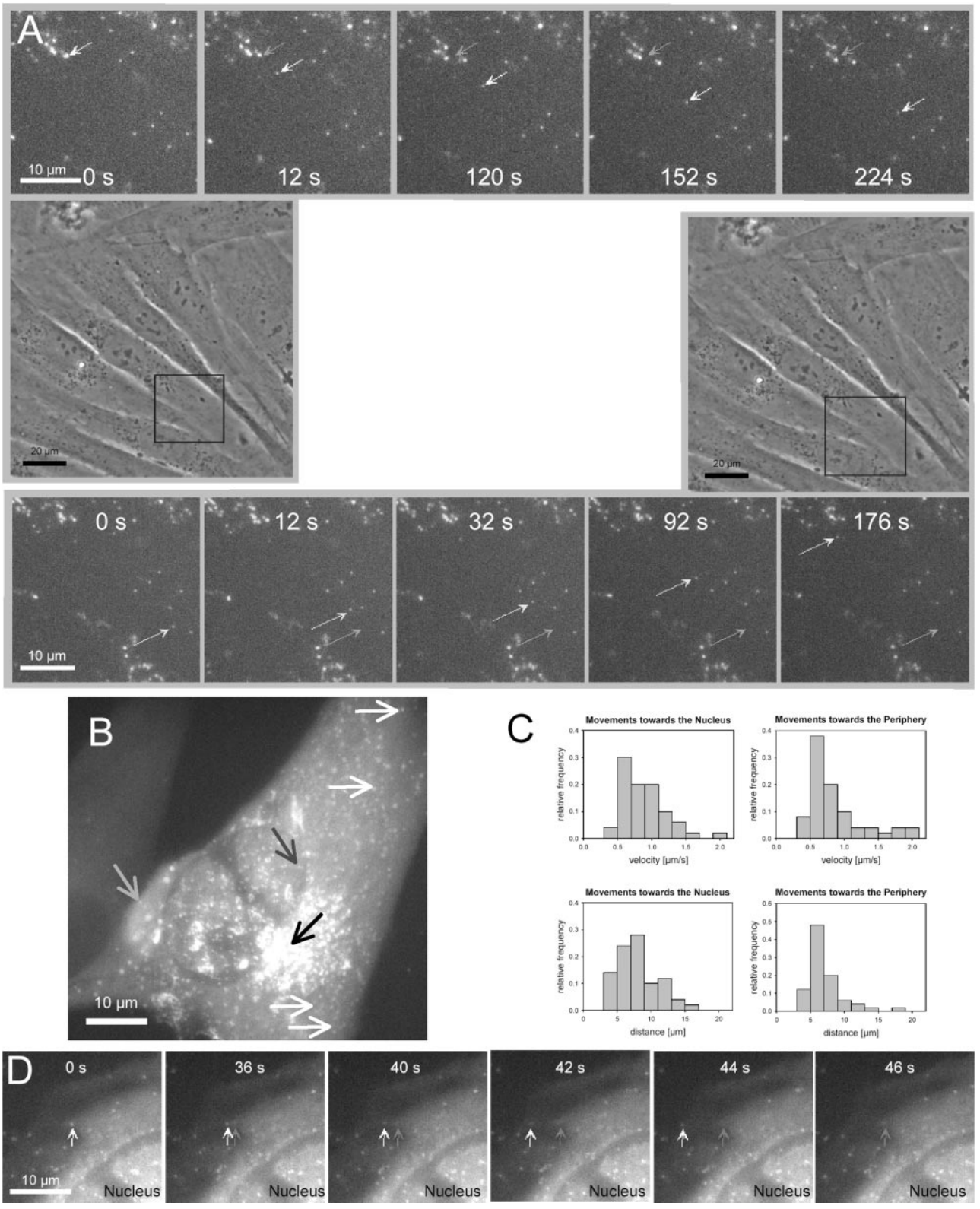

FIG. 5. Live imaging of particle movements in fibroblasts infected by UL32-EGFP-HCMV-TB40 as documented by time-lapse fluorescence microscopy. (A) Centripetal and centrifugal movements in fibroblasts 1 h after infection at an MOI of 10. White arrows, actual position of the particle; gray arrows, starting point of the particle. Selected frames from videos are shown. (B) Particle movements in an infected cell at 4 days after infection at an MOI of 0.1. The light gray arrow points to a particle moving parallel to the cell margin. The black arrow points to the perinuclear aggregation site. The dark gray arrow indicates the starting point of a particle appearing to be leaving the nucleus. The paired white arrows indicate routes of saltatory movements. (C) Statistical analysis of particle movements in fibroblasts 3 days after infection with UL32-EGFP-HCMV-TB40. (D) Time-lapse series suggestive of release of a particle at the cell periphery of a fibroblast at 4 days after infection at an MOI of 0.1. Selected frames from a video are shown.

after about 2 days of infection, when progeny virus appeared, and at a late stage of infection when numerous progeny virus particles were present. During the initial phase of high-dose infections (MOI = 10), both centripetal and centrifugal saltatory movements could be observed with a subset of input particles, whereas most input particles performed irregular movements at their position (Fig. 5A and data not shown). Although no predominance of centripetal movements was found in fibroblasts during observation periods of about 500 s, an overall aggregation of particles at perinuclear sites occurred after several hours. At about 2 days after low-dose infection, the number of particles within infected cells increased, reflecting the generation of progeny virus. Emerging virus particles were first located in the inclusions of the nucleus but were soon also detectable within the cytoplasm (Fig. 4), where they aggregated at perinuclear sites during late stages of infection.

During the late stage of infection, all kinds of movement as characterized for the initial phase of infection were also present (Fig. 5B and data not shown). In particular, particles seemed not to be destined for efficient egress from the cell. A subset of particles reached the periphery of the cell by irregular movements rather than by directed long-distance movements. Some of these particles performed back-and-forth movements parallel to the cell margins. However, during a 300-s observation sequence with a time frame of 2 s, events suggestive of particle release were a rare singular finding (Fig. 5D and data not shown). Moreover, when late-stage infected cells were cocultured with an excess of uninfected cells, cell-to-cell transmission also could not be demonstrated unequivocally within sequences of 300 s at a time frame of 2 s although numerous particles were produced by these late-stage infected cells (data not shown). Together these findings strongly indicated that release of virions from late-stage infected cells is not a directed efficient process that would apply for the majority of cytoplasmic particles. In summary, various kinds of short-distance or long-distance movements with different directions occurred simultaneously throughout the viral life cycle without a clear predominance of a certain pattern at any time point.

DISCUSSION

Proper translocations within infected cells are critical events at various points during the replication cycle of viruses. In particular this applies to herpesviruses, which are known to replicate their DNA and assemble their 100-nm large capsids in the nuclei of infected cells. Thus, successful herpesviral replication depends on penetration into the cell across the actin cortex, centripetal transport towards the nucleus, egress of viral progeny capsids from the nucleus, centrifugal transport towards the cell periphery, and egress through the cell cortex. At present, most of these events are poorly understood. Although general shifts in the number and location of virus particles can be documented by the staining of fixed infected-cell cultures at different time points after infection, there are limitations of such an approach that will prevent more detailed insights. In particular, analyses of fixed cell cultures do not allow for (i) sequential analyses of a single cell, (ii) tracking of individual virus particles, and (iii) documentation of narrow time frames. Such information can best be achieved by live analysis of cells infected by fluorescence-tagged virus. Here we report the generation of green fluorescent human cytomegalovirus particles expressing the tegument protein pp150 (UL32) as an EGFP fusion protein.

As a target for EGFP fusion, we chose the viral tegument protein pp150 (UL32) for several reasons. We had successfully stained virus particles during viral entry and nuclear transport by indirect immunostaining of pUL32 (25). Evidence from biochemical binding studies indicated that pUL32 binds directly and strongly to capsids (1, 2). Steric constraints caused by an EGFP tag were expected to be better tolerated when EGFP was fused to a capsid-associated tegument protein rather than to a capsid protein itself. As pUL32 binds to the capsid through its amino one-third (1), the carboxy terminus was expected to be free and appeared to be an ideal target for EGFP fusion. In order to cause as little alteration of the viral genome as possible, the EGFP gene was fused to the UL32 gene directly before the last codon at the autologous position without introducing any further selection marker. Microinjection of a purified recombination fragment (consisting of the UL32 open reading frame truncated by one codon, the coding sequence of EGFP, and 1,622 bp of the UL31 open reading frame) into infected fibroblasts during the early phase of replication resulted in the appearance of green fluorescent foci of infected cells, from which recombinant UL32-EGFP-HCMV-TB40 could be enriched by three sequential plaque purifications. Limiting-dilution infections with plaque-purified virus preparations and subsequent simultaneous immunofluorescence of pUL32 and EGFP revealed that all infectious units within the preparation expressed EGFP. Immunoblotting of virion proteins of UL32-EGFP-HCMV-TB40 with a pUL32-specific antibody demonstrated the lack of wild-type pUL32 and the expected shift of the fusion protein towards a higher apparent molecular weight. Enzymatic DNA amplification with wild-type-specific sequences further confirmed that plaque-purified preparations of UL32-EGFP-HCMV-TB40 were free of contaminating infectious wild-type virus.

The recombinant UL32-EGFP-HCMV-TB40 appears to express viral proteins and produce progeny virus with kinetics and titers similar to those of wild-type HCMV TB40. In particular, pUL32-EGFP is expressed with the same kinetics and with the same subcellular localization as wild-type pUL32, and all EGFP signals are colocalized with pUL32 signals. Infectious progeny virions released from infected cells displayed green fluorescence when analyzed as free extracellular particles and during adsorption and entry in fibroblast cultures. Ultrastructural immunogold analyses demonstrated the incorporation of pUL32-EGFP into progeny virion particles. In conclusion, fusion of EGFP to the carboxy terminus of HCMV-pUL32 was successful and resulted in green fluorescent HCMV with growth properties that were indistinguishable from those of wild-type virus. When applied in live-imaging approaches, this virus will enable live analyses of various kinds of translocations of viral particles during the replicative cycle.

As a first application of UL32-EGFP-HCMV-TB40, we have analyzed the kinetics and localization of acquisition of pUL32 by newly synthesized HCMV particles during the late phase of infection. Surprisingly, the first pUL32-containing particles appeared within the nucleus, indicating that binding of pUL32 to the capsid is an early step of the tegumentation, which occurs

before particles reach the nuclear membrane or lamina. The lack of nuclear pUL32 signals in an earlier study (24) might be due to limited sensitivity of the staining technique or to the usage of antibodies that might miss the nuclear form of pUL32. Consistent with our results, the nuclear localization of pUL32 has been demonstrated by Hensel et al. (9). In principle, pUL32 might thus be important for any of the subsequent steps, including transportation towards the nuclear lamina, egress from the nucleus, and regulation of the following tegumentation events within the cytoplasm. Targeted introduction of mutations into the pUL32 part of the UL32-EGFP fusion gene will now allow for a detailed analysis of pUL32 functions in the context of viral morphogenesis and egress.

In addition, we have analyzed the intracellular movements of green fluorescent particles during the late phase of infection, when morphogenesis and egress from the infected cell take place. Again the results were surprising, as time-lapse series of micrographs indicated a variety of different particle movements with an almost chaotic appearance rather than the predominance of any directed translocation pattern. In particular, most particles within the cytoplasm performed short-distance back-and-forth or irregular movements, while a smaller fraction of particles performed centripetal and centrifugal long-distance movements or moved along the margins of the infected cell. Only very few events suggestive of particle release at the cell borders have been documented. Taken together, the particle movements observed in productively infected cells do not support the assumption of an effective egress of progeny virus during the late stage of infection. Rather, release of virus by infected cells seems to be a rare event. It is noteworthy, however, that this is in concordance with the quantitative aspects of HCMV production by infected-cell cultures. A culture of 4×10^6 late-stage infected fibroblasts produces about 10^8 infectious units per day, which corresponds to about 1 infectious unit per cell per h. On the basis of this calculation it is not surprising that release of green fluorescent particles from infected cells was a rare event in our analysis.

Regarding the nature of the movements that were observed, the short-distance movements performed by the majority of particles could reflect active transportation of particles by the cellular transport machinery, movements of cellular vesicles associated with virus capsids during the process of tegumentation and envelopment, or passive Brownian dynamics along with the surrounding cytoplasm. The long-distance movements cannot be explained by passive movements together with the surrounding cytoplasm but are reminiscent of active transportation along microtubular structures with regard to their mean apparent velocity of about 0.7 to 0.8 μm/s and peak velocities of 2 μm/s. In nerve axons, higher mean velocities of about 2 μm/s have been reported for pseudorabies virus (27). In the cytoplasm of epithelial cells, however, adenoviruses moved at a velocity of about 0.5 μm/s, with peak velocities of about 2 μm/s in both directions (31). Likewise, vaccinia viruses were reported to move in epithelial cells at velocities of about 0.5 μm/s (7). In an in vitro system the velocities of microtubule-based dynein-mediated and kinesin-mediated transport were 0.7 and 1.0 μm/s, respectively (13). The movements described here for EGFP-tagged HCMV particles are therefore consistent with the assumption of microtubule-based motility. Although it is unclear whether naked capsids or enveloped particles are transported, this indicates that the virus might use the cellular transportation machinery in order to reach the periphery of the cell. Whereas a number of particles actually are translocated towards the cell periphery and particle movements along the cell margins were frequently detected, egress from the cell seems to be inefficient. It will now be interesting to study whether egress from the cytoplasm is hampered by the physical barrier formed by actin cortex or by difficulties performing the energy-consuming fusion of membranes.

In summary, a green fluorescent HCMV variant is now available, enabling live analyses of viral particle translocations during various steps of the viral replication cycle. From such descriptive studies novel aspects of HCMV entry and morphogenesis will arise and can be subjected to detailed cell-biological or biochemical analyses in the future.

ACKNOWLEDGMENT

This work was supported by the German Research Foundation (grants SI 779/2–1 and SI 779/3–1).

REFERENCES

1. **Baxter, M. K., and W. Gibson.** 2001. Cytomegalovirus basic phosphoprotein (pUL32) binds to capsids in vitro through its amino one-third. J. Virol. **75:**6865–6873.
2. **Benko, D. M., R. S. Haltiwanger, G. W. Hart, and W. Gibson.** 1988. Virion basic phosphoprotein from human cytomegalovirus contains O-linked N-acetylglucosamine. Proc. Natl. Acad. Sci. USA **85:**2573–2577.
3. **Danscher, G.** 1981. Histochemical demonstration of heavy metals. A revised version of the sulphide silver method suitable for both light and electron-microscopy. Histochemistry **71:**1–16.
4. **Desai, P., and S. Person.** 1998. Incorporation of the green fluorescent protein into the herpes simplex virus type 1 capsid. J. Virol. **72:**7563–7568.
5. **Döhner, K., A. Wolfstein, U. Prank, C. Echeverri, D. Dujardin, R. Vallee, and B. Sodeik.** 2002. Function of dynein and dynactin in herpes simplex virus capsid transport. Mol. Biol. Cell **13:**2795–2809.
6. **Elliott, G., and P. O'Hare.** 1999. Live-cell analysis of a green fluorescent protein-tagged herpes simplex virus infection. J. Virol. **73**:4110–4119.
7. **Geada, M. M., I. Galindo, M. M. Lorenzo, B. Perdiguero, and R. Blasco.** 2001. Movements of vaccinia virus intracellular enveloped virions with GFP tagged to the F13L envelope protein. J. Gen. Virol. **82:**2747–2760.
8. **Goodrum, F. D., C. T. Jordan, K. High, and T. Shenk.** 2002. Human cytomegalovirus gene expression during infection of primary hematopoietic progenitor cells: a model for latency. Proc. Natl. Acad. Sci. USA **99:**16255–16260.
9. **Hensel, G., H. Meyer, S. Gartner, G. Brand, and H. F. Kern.** 1995. Nuclear localization of the human cytomegalovirus tegument protein pp150 (ppUL32). J. Gen. Virol. **76:**1591–1601.
10. **Isomura, H., and M. F. Stinski.** 2003. The human cytomegalovirus major immediate-early enhancer determines the efficiency of immediate-early gene transcription and viral replication in permissive cells at low multiplicity of infection. J. Virol. **77:**3602–3614.
11. **Iwata, M., J. Vieira, M. Byrne, H. Horton, and B. Torok Storb.** 1999. Interleukin-1 (IL-1) inhibits growth of cytomegalovirus in human marrow stromal cells: inhibition is reversed upon removal of IL-1. Blood **94:**572–578.
12. **Kerman, I. A., L. W. Enquist, S. J. Watson, and B. J. Yates.** 2003. Brainstem substrates of sympatho-motor circuitry identified using trans-synaptic tracing with pseudorabies virus recombinants. J. Neurosci. **23:**4657–4666.
13. **King, S. J., and T. A. Schroer.** 2000. Dynactin increases the processivity of the cytoplasmic dynein motor. Nat. Cell Biol. **2:**20–24.
14. **Mabit, H., M. Y. Nakano, U. Prank, B. Saam, K. Dohner, B. Sodeik, and U. F. Greber.** 2002. Intact microtubules support adenovirus and herpes simplex virus infections. J. Virol. **76:**9962–9971.
15. **Mahy, B. W. J., and H. O. Kangro.** 1996. Virology methods manual. Academic Press, San Diego, Calif.
16. **Marschall, M., M. Freitag, S. Weiler, G. Sorg, and T. Stamminger.** 2000. Recombinant green fluorescent protein-expressing human cytomegalovirus as a tool for screening antiviral agents. Antimicrob. Agents Chemother. **44:**1588–1597.
17. **Mettenleiter, T. C.** 2002. Herpesvirus assembly and egress. J. Virol. **76:**1537–1547.
18. **Mocarski, E. S. J., and C. T. Courcelle.** 2001. Cytomegaloviruses and their replication, p. 2629–2674. *In* D. M. Knipe and P. M. Howley (ed.), Fields virology, 4th ed., vol. 2. Lippincott Williams & Wilkins, Philadelphia, Pa.

19. **Muranyi, W., J. Haas, M. Wagner, G. Krohne, and U. H. Koszinowski.** 2002. Cytomegalovirus recruitment of cellular kinases to dissolve the nuclear lamina. Science **297:**854–857.
20. **Murphy, E. A., D. N. Streblow, J. A. Nelson, and M. F. Stinski.** 2000. The human cytomegalovirus IE86 protein can block cell cycle progression after inducing transition into the S phase of permissive cells. J. Virol. **74:**7108–7118.
21. **Potel, C., K. Kaelin, I. Gautier, P. Lebon, J. Coppey, and F. Rozenberg.** 2002. Incorporation of green fluorescent protein into the essential envelope glycoprotein B of herpes simplex virus type 1. J. Virol. Methods **105:**13–23.
22. **Pyner, S., J. Cleary, P. M. Buchan, and J. H. Coote.** 2001. Tracing functionally identified neurons in a multisynaptic pathway in the hamster and rat using herpes simplex virus expressing green fluorescent protein. Exp. Physiol. **86:**695–702.
23. **Sanchez, V., C. L. Clark, J. Y. Yen, R. Dwarakanath, and D. H. Spector.** 2002. Viable human cytomegalovirus recombinant virus with an internal deletion of the IE2 86 gene affects late stages of viral replication. J. Virol. **76:**2973–2989.
24. **Sanchez, V., K. D. Greis, E. Sztul, and W. J. Britt.** 2000. Accumulation of virion tegument and envelope proteins in a stable cytoplasmic compartment during human cytomegalovirus replication: characterization of a potential site of virus assembly. J. Virol. **74:**975–986.
25. **Sinzger, C., M. Kahl, K. Laib, K. Klingel, P. Rieger, B. Plachter, and G. Jahn.** 2000. Tropism of human cytomegalovirus for endothelial cells is determined by a post-entry step dependent on efficient translocation to the nucleus. J. Gen. Virol. **81:**3021–3035.
26. **Sinzger, C., K. Schmidt, J. Knapp, M. Kahl, R. Beck, J. Waldman, H. Hebart, H. Einsele, and G. Jahn.** 1999. Modification of human cytomegalovirus tropism through propagation in vitro is associated with changes in the viral genome. J. Gen. Virol. **80:**2867–2877.
27. **Smith, G. A., S. P. Gross, and L. W. Enquist.** 2001. Herpesviruses use bidirectional fast-axonal transport to spread in sensory neurons. Proc. Natl. Acad. Sci. USA **98:**3466–3470.
28. **Sodeik, B., M. W. Ebersold, and A. Helenius.** 1997. Microtubule-mediated transport of incoming herpes simplex virus 1 capsids to the nucleus. J. Cell Biol. **136:**1007–1021.
29. **Stierhof, Y. D., B. M. Humbel, and H. Schwarz.** 1991. Suitability of different silver enhancement methods applied to 1 nm colloidal gold particles: an immunoelectron microscopic study. J. Electron Microsc. Technol. **17:**336–343.
30. **Strive, T., E. Borst, M. Messerle, and K. Radsak.** 2002. Proteolytic processing of human cytomegalovirus glycoprotein B is dispensable for viral growth in culture. J. Virol. **76:**1252–1264.
31. **Suomalainen, M., M. Y. Nakano, S. Keller, K. Boucke, R. P. Stidwill, and U. F. Greber.** 1999. Microtubule-dependent plus- and minus end-directed motilities are competing processes for nuclear targeting of adenovirus. J. Cell Biol. **144:**657–672.